Materials Transactions, Vol. 48, No. 9 (2007) pp. 2304 to 2311
Special Issue on Solidification Science and Processing for Advanced Materials

Prediction of Thermal Properties In A Solidification Process

Yu-Ru Chen*[1], Long-Sun Chao and Li-Sheng Lin*[2]

Department of Engineering Science, National Cheng Kung University, No. 1, Ta-Hsueh Road, Tainan 701, Taiwan, R. O. China

In solidification models, the uncertainty of thermal properties will influence the computing results. In this paper, a non-linear inverse method is proposed to predict the thermal properties of materials according to the temperature data measured in solidification processes. With the proposed method, the solid and liquid thermal conductivities and specific heats of materials can be computed simultaneously. Furthermore, with the effective specific heat method, the inverse scheme can be utilized to calculate the latent heat. Stefan and Neumann problems are used to test the proposed method. From the computing results, it is proved that the properties can be predicted accurately. After that, the method is applied to the casting experiments, in which Al, Sn, 90 mass% Sn-10 mass% Pb alloy and A356 aluminum alloy are taken as testing materials. The computed thermal properties are very close to the values reported in the literature. From these results, it is shown that the proposed method provides an easy way to predict thermal properties with simple casting experiments. [doi:10.2320/matertrans.MB200712]

(Received March 2, 2007; Accepted April 26, 2007; Published July 11, 2007)

Keywords: *thermal conductivity, specific heat, latent heat, non-linear inverse model, solidification*

1. Introduction

In the solidified analysis, the temperature variation will directly affect the microstructures of the materials that are vitally related to their qualities. In the analysis, the thermal properties used are thermal conductivity, specific heat, latent heat and so on. The thermal analysis cannot proceed without those properties. The thermal properties could often be found in the literature. If the properties cannot be obtained, the experiment method needs to be used to acquire them. However, the equipments are generally not cheap or the experimental environment is severe, and therefore the properties cannot be obtained easily. In this work, a simple casting experiment with the proposed inverse method is used to predict the thermal properties of the casting material.

To predict the thermal properties, inverse methods are often combined with experiments. In the inverse study of the thermal conductivity, Kitamura *et al.*[1)] and Chen[2)] regarded it as the function of time and space and used the distributed parameter system to predict its value. Huang and Ozisik[3)] utilized the Direct Integration and the Levenberg-Marquardt method to estimate the thermal conductivity in a one-dimensional heat transfer environment and applied the related error of the statistics to analyze the reliability. Alifanov *et al.*[4,5)] used the function prediction method and Huang[6)] utilized the conjugate gradient algorithm of the function prediction to solve the inverse problem of the heat transfer. Chen *et al.*[7–9)] applied the mixed Laplace transform to solve the linear and non-linear problem of the transient heat transfer. Zhong[10)] used Pehlke and Powell's method to calculate the thermal diffusion coefficient of the aluminum alloy. Yang[11,12)] re-arranged the matrix equation of the heat transfer problems for liner inverse problems to calculate the heat source and the thermal conductivities. Those researches stated above include the predictions of the boundary conditions (of temperature or heat flux) and the thermal physical properties such as specific heat and thermal conductivity. However, few studies worked on the prediction of the latent heat. For example, Upadhya *et al.*[13)] used the cooling curves to estimate the latent heat of metals. Kwok[14)] used Yang's method to compute the thermal conductivity inversely and built a method to predict the latent heat based on the Stefan condition.

This paper took the Yang's method[11)] as the foundation, and small variation concept was added to compute the solid and liquid thermal conductivities and specific heat of materials simultaneously. The iterative process in the computation cannot be avoided since the resulting inverse problem was not linear. With the effective specific heat method, the inverse scheme was further utilized to calculate the latent heat. In this work, the Stefan and Neumann problems were used to test the proposed model. After the test, the model was applied to predict the thermal properties from the designed casting experiments.

2. Solidification Models

This paper uses the proposed inverse numerical method with the designed casting experiment to predict the thermal properties of the casting metals. Before the proposed method is applied to real casting experiments, numerical experiments are firstly utilized to prove the feasibility of the method by using the Stefan and Neumann problem.[15)] From the exact solutions of the problems with given thermal conductivities, specific heats and latent heat, the measured temperatures are taken to inversely predict the thermal properties, which are compared with the given ones. The two solidification problems, Stefan and Neumann problems, are described as follows.

2.1 Stefan problem

The physical model covers a one-dimensional semi-infinite region, as shown in Fig. 1. The initial pouring temperature is melting point temperature T_f. When $t \geq 0$, the temperature at $x = 0$ is equal to T_m, which represents the mold temperature. The solidification process proceeds from the left to the right. $s(t)$ is the position of solid-liquid interface.

In the problem, the basic assumptions are

*[1]Ph.D. Student, National Cheng Kung University
*[2]Graduated Student, National Cheng Kung University

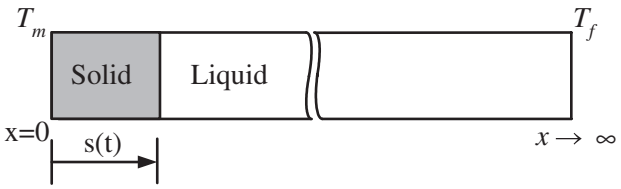

Fig. 1 Schematic diagram of the Stefan Problem.

(1) The thermal properties are constant.
(2) The effect of natural convection is ignored.

According to the model and assumptions described above, only the temperature field of the solid phased needs to be solved. Its energy equation, initial condition, and boundary conditions can be written as follows.

$$\rho_s Cp_s \frac{\partial T}{\partial t} = k_s \nabla^2 T \tag{1}$$

$$T(x, t = 0) = T_f \tag{2}$$

$$T_s(x, 0) = T_m \tag{3}$$

At the solid/liquid interface ($x = s(t)$),

$$T = T_f \tag{4}$$

$$k_s \frac{\partial T_s}{\partial x} = \rho L_f \frac{ds(t)}{dt} \tag{5}$$

where L_f is the latent heat. The analytical solution of the problem is

$$T = T_m + \frac{T_f - T_m}{erf(\gamma)} erf\left(\frac{x}{\sqrt{4\alpha_s t}}\right) \tag{6}$$

$$s(\tau) = 2\gamma\sqrt{\alpha_s t} \tag{7}$$

where α_s is the thermal diffusivity of solid. γ is a constant and can be calculated by the following equation

$$\gamma e^{\gamma^2} erf(\gamma) = \frac{(T_f - T_m)Cp_s}{L_f\sqrt{\pi}} \tag{8}$$

2.2 Neumann problem

The temperature distribution of the Stefan problem is similar to that of the real solidification of the pure metal. However, since the pouring temperature is the melting temperature and there is not temperature variation in the liquid, the inverse method cannot predict the liquid properties. Consequently, the Neumann problem is used to compensate this shortage.

The physical model of the Neumann covers a one-dimensional semi-infinite region, which is the same as that of the Stefan problem. The pouring temperature T_p can be larger than T_f and the mold temperature T_m is zero. The basic assumptions are the same as those of the Stefan problem. Hence, the governing equation, initial condition, and boundary condition can be written as follows.

$$\rho_s Cp_s \frac{\partial T_s}{\partial t} = k_s \nabla^2 T_s \tag{9}$$

$$\rho_l Cp_l \frac{\partial T_l}{\partial t} = k_l \nabla^2 T_l \tag{10}$$

$$T_l(x, t = 0) = T_p \tag{11}$$

$$T_s(x, 0) = T_m \tag{12}$$

At the solid/liquid interface ($x = s(t)$),

$$T_s = T_l = T_f \tag{13}$$

$$k_s \frac{\partial T_s}{\partial x} - k_l \frac{\partial T_l}{\partial x} = \rho L_f \frac{ds(t)}{dt} \tag{14}$$

As x approached the infinity,

$$T_l = T_p \tag{15}$$

The analytical solution of the Neumann problem is

$$T_s = \frac{T_f}{erf(\gamma)} erf\left(\frac{x}{\sqrt{4\alpha_s t}}\right) \tag{16}$$

$$T_l = T_p - \frac{T_p - T_f}{erfc(\gamma(\sqrt{\alpha_s/\alpha_l})} erfc\left(\frac{x}{\sqrt{4\alpha_l t}}\right) \tag{17}$$

$$s(t) = 2\gamma\sqrt{\alpha_s t} \tag{18}$$

where α_l is the thermal diffusivity of liquid. γ is a constant and can be calculated by the following equation

$$\frac{\exp(-\gamma^2)}{erf(\gamma)} - \frac{k_l}{k_s}\frac{\sqrt{\alpha_s}}{\sqrt{\alpha_l}} \frac{(T_p - T_f)\exp\left(-\gamma^2\frac{\alpha_s}{\alpha_l}\right)}{T_f erfc(\gamma\sqrt{\alpha_s/\alpha_l})} = \frac{\gamma L_f\sqrt{\pi}}{T_f Cp_s} \tag{19}$$

3. Numerical Method of the Direct Problem

The direction problem of the inverse method is the axial heat transfer of the cylindrical casting and its governing equation can be written as

$$Cp\frac{\partial T}{\partial t} = \frac{\partial}{\partial x}\left(k\frac{\partial T}{\partial x}\right) \tag{20}$$

where Cp is the specific heat and k is the thermal conductivity of the casting. If the thermal conductivity is a function of temperature, the energy equation is nonlinear and can be expanded as

$$Cp\frac{\partial T}{\partial t} = \frac{\partial k}{\partial x}\frac{\partial T}{\partial x} + k\frac{\partial^2 T}{\partial x^2} \tag{21}$$

In the work, the numerical method is the finite difference method. In the formulation of the difference equation, the centered difference is utilized for the space derivative and the backward difference is for the time derivative. Accordingly, the finite-difference formulation of the governing equation can be written as

$$Cp\frac{T_i^{n+1} - T_i^n}{\Delta t} = \frac{k_{i+1}^{n+1} - k_{i-1}^{n+1}}{2\Delta x}\frac{T_{i+1}^{n+1} - T_{i-1}^{n+1}}{2\Delta x} + k_i^{n+1}\frac{T_{i+1}^{n+1} - 2T_i^{n+1} + T_{i-1}^{n+1}}{(\Delta x)^2} \tag{22}$$

By applying the equation to the interior nodes of the computing domain with the difference equations on the boundaries, a matrix equation of the nodal temperatures can be arranged as

$$[A]\{T^{n+1}\} = \{T^n\} \tag{23}$$

where [A] is the coefficient matrix. $\{T^{n+1}\}$ and $\{T^n\}$ are the columnar matrices of nodal temperatures at time step $n+1$ and n, respectively. Equation (23) is the basic equation for the inverse method stated below.

4. Inverse Method for Thermal Conductivity and Specific Heat

In this work, an estimated model was built to predict the specific heat and thermal conductivity simultaneously by solving the nonlinear system equations iteratively with the measured temperatures of the interior points in the casting. The implicit finite difference formulation was applied to the energy equation combined with the unknown properties. At first, setting the basic equations of the iterative computations as below,

$$Cp_{m+1} = Cp_m + \Delta Cp \tag{24}$$

$$k_{m+1} = k_m + \Delta k \tag{25}$$

$$T_{m+1} = T_m + \Delta T \tag{26}$$

where Cp, k and T are the columnar matrices of the specific heat, thermal conductivity and temperature. ΔCp and Δk are the small variations of Cp and k. ΔT is the small variation caused by ΔCp and Δk. m is the iteration number.

The energy equation can be discretized to obtain the matrix equation of the direct sub-problem, which is the same as eq. (23) and is rewritten as

$$IT_m = J \tag{27}$$

where I is the coefficient matrix and J is the matrix of given conditions.

If the specific heat matrix becomes $Cp + \Delta Cp$, the corresponding temperature becomes $T + \Delta T$ and the corresponding governing equation can be given by

$$(Cp + \Delta Cp)\frac{\partial(T + \Delta T)}{\partial t} = k\frac{\partial^2(T + \Delta T)}{\partial x^2} \tag{28}$$

By ignoring the high order term, the equation can be rewritten as

$$k\frac{\partial^2(\Delta T)}{\partial x^2} - Cp\frac{\partial(\Delta T)}{\partial t} = \Delta Cp\frac{\partial T}{\partial t} \tag{29}$$

With the same difference scheme used in eq. (22), the difference equation of eq. (29) can be given by

$$k\frac{\Delta T_{i-1}^{n+1} - 2\Delta T_i^{n+1} + \Delta T_{i+1}^{n+1}}{\Delta x^2} - Cp\frac{\Delta T_i^{n+1} - \Delta T_i^n}{\Delta t} = \Delta Cp\frac{T_i^{n+1} - T_i^n}{\Delta t} \tag{30}$$

The corresponding matrix equation for all the space grid points and time steps can be written as

$$L\Delta T = M\Delta Cp \tag{31}$$

where

$$\Delta Cp = \{\Delta Cp\} \tag{32}$$

$$M = \{M_2^1, M_3^1, \ldots, M_{nx-1}^1, \ldots, M_2^{nt}, M_3^{nt}, \ldots, M_{nx-1}^{nt}\}^T \tag{33}$$

$$M_i^{n+1} = (T_i^{n+1} - T_i^n)/Cp \tag{34}$$

$$\Delta T = \{\Delta T_2^1, \Delta T_3^1, \ldots, \Delta T_{nx-1}^1, \ldots, \Delta T_2^{nt}, \Delta T_3^{nt}, \ldots \Delta T_{nx-1}^{nt}\}^T \tag{35}$$

$$L_{ij} = \begin{cases} \dfrac{\Delta t}{\Delta x^2}\dfrac{k}{Cp} & j = i+1 \text{ or } i-1 \\ -2\dfrac{\Delta t}{\Delta x^2}\dfrac{k}{Cp} - 1 & j = i \\ 1 & j = i - (nx-2) \\ 0 & \text{others} \end{cases} \tag{36}$$

If the thermal conductivity matrix becomes $k + \Delta k$, the corresponding temperature becomes $T + \Delta T$ and the corresponding governing equation can be given by

$$Cp\frac{\partial(T + \Delta T)}{\partial t} = (k + \Delta k)\frac{\partial^2(T + \Delta T)}{\partial x^2} \tag{37}$$

By ignoring the high order term, the equation can be rewritten as

$$Cp\frac{\partial(\Delta T)}{\partial t} - k\frac{\partial^2(\Delta T)}{\partial x^2} = \Delta k\frac{\partial^2(T)}{\partial x^2} \tag{38}$$

The difference equation of eq. (38) can be given by

$$Cp\frac{\Delta T_i^{n+1} - \Delta T_i^n}{\Delta t} - k\frac{\Delta T_{i-1}^{n+1} - 2\Delta T_i^{n+1} + \Delta T_{i+1}^{n+1}}{(\Delta x)^2} = \Delta k\frac{T_{i-1}^{n+1} - 2T_i^{n+1} + T_{i+1}^{n+1}}{(\Delta x)^2} \tag{39}$$

The corresponding matrix equation for all the space grid points and time steps can be written as

$$N\Delta T = O\Delta k \tag{40}$$

where

$$\Delta k = \{\Delta k\} \tag{41}$$

$$O = \{O_2^1, O_3^1, \ldots, O_{nx-1}^1, \ldots, O_2^{nt}, O_3^{nt}, \ldots O_{nx-1}^{nt}\}^T \tag{42}$$

$$O_i^{n+1} = \frac{\Delta t(T_{i-1}^{n+1} - 2T_i^{n+1} + T_{i+1}^{n+1})}{Cp(\Delta x)^2} \tag{43}$$

$$\Delta T = \{\Delta T_2^1, \Delta T_3^1, \ldots, \Delta T_{nx-1}^1, \ldots, \Delta T_2^{nt}, \Delta T_3^{nt}, \ldots \Delta T_{nx-1}^{nt}\}^T \tag{44}$$

$$N_{ij} = \begin{cases} \dfrac{\Delta t}{\Delta x^2}\dfrac{k}{Cp} & j = i+1 \text{ or } i-1 \\ 2\dfrac{\Delta t}{\Delta x^2}\dfrac{k}{Cp} + 1 & j = i \\ 1 & j = i - (nx-2) \\ 0 & \text{others} \end{cases} \tag{45}$$

With eq. (31) and (40), the calculation procedures of thermal conductivity and specific heat are

1. Give the initial guesses of thermal conductivity and specific heat, Cp_0 and k_0.
2. The components of ΔT are the differences between the measured temperatures and the computed ones with the initial or modified thermal conductivity and specific heat.
3. From eq. (31) and (40), ΔCp_{m+1} and Δk_{m+1} can be obtained by applying the Yang's method.[11] Repeat the step 2 and 3 until the convergent values of thermal conductivity and specific heat are obtained.

5. Prediction of Latent Heat

In this paper, the effective specific heat method[16] is used for the prediction of latent heat. In the method, the relationship between the effective specific heat Cp^{eff} and temperature of pure metal can be given as

$$Cp^{eff} = \begin{cases} Cp_{\mathrm{L}} & T > T_f + \Delta T^* \\ \dfrac{1}{2}\left(\dfrac{L_f}{\Delta T^*} + Cp_{\mathrm{L}} + Cp_s\right) & T_f - \Delta T^* \le T \le T_f + \Delta T^* \\ Cp_s & T < T_f - \Delta T^* \end{cases} \tag{46}$$

where T_{f} is the melting temperature and $2 \times \Delta T^*$ represents the size of the artificial mushy zone, as shown in Fig. 2. The energy equation for this method can be written as

$$Cp^{eff}\frac{\partial T}{\partial t} = \frac{\partial}{\partial x}\left(k\frac{\partial T}{\partial x}\right) \tag{47}$$

In the prediction of latent heat, Cp_{S} and Cp_{L} are assumed to be known and then the latent heat can be calculated by using the Yang's inverse method to estimate the value of Cp^{eff}.

6. Numerical and Casting Experiments

Before the proposed method is applied to real casting experiments, numerical experiments are firstly utilized to prove the feasibility of the method by using the Stefan and Neumann problems. From the exact solutions of the problems with given thermal conductivities, specific heats and latent heat, the measured temperatures are taken to predict the thermal properties, which are compared with the given ones.

After the numerical experiments, a casting process in a vertical thermal-insulated mold was used for the proposed inverse method, which is shown in Fig. 3. Because this experimental model is to simulate the phenomenon of one-dimensional heat transfer, a heating coil is wound around the mold to reduce the radial heat transfer and the bottom water-cooling copper chill is used to enhance the axial heat transfer. Thermal couples are installed along the mold centerline and near the chill. With the proposed method, the measured temperatures of those thermal couples are utilized to estimate the thermal properties, which are compared with those from the literature.

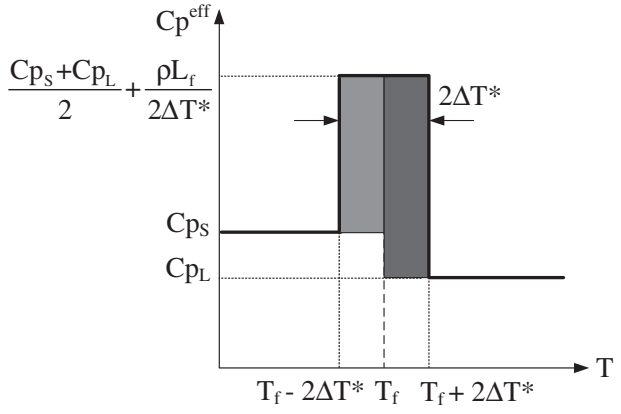

Fig. 2 The relationship between effective specific heat and temperature of pure metal.

7. Results and Discussions

In this work, two numerical experiments is used to test the proposed method by taking the measured temperatures from the exact solutions of the Stefan and Neumann problems to predict thermal conductivities, specific heats and latent heat. After that, a vertical thermal-insulated mold with a bottom chill is utilized to simulate the one-dimensional heat transfer of a casting process. The measured temperatures in the metal during the casting process are used to estimate the thermal properties. The computing results of the proposed method are shown as follows.

7.1 The results of the numerical experiments

7.1.1 Numerical experimental results of Stefan problem

This experiment takes the temperature data from the Stefan problem to estimate the thermal properties of solid, which are assumed to be constant in the problem and the inverse calculation. The domain of Stefan problem is semi-infinite. This work chooses ten successive grid points from the domain, whose temperature data are used in the inverse calculation.

In this experiment, it is expected that the way of taking temperature data will work for the inverse method and the real casting experiment. However, the boundary condition of

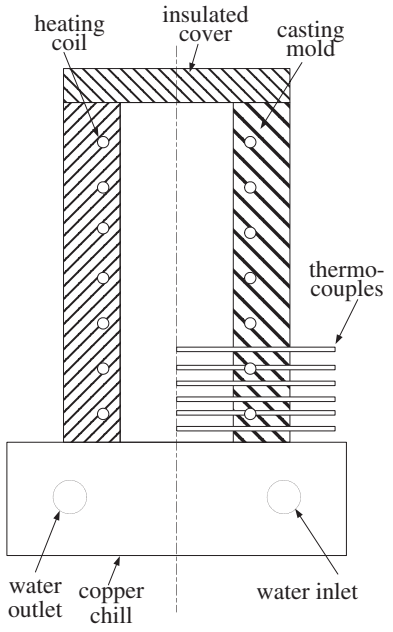

Fig. 3 Schematic diagram of vertical casting mold with heating coil and water-cooling copper chill.

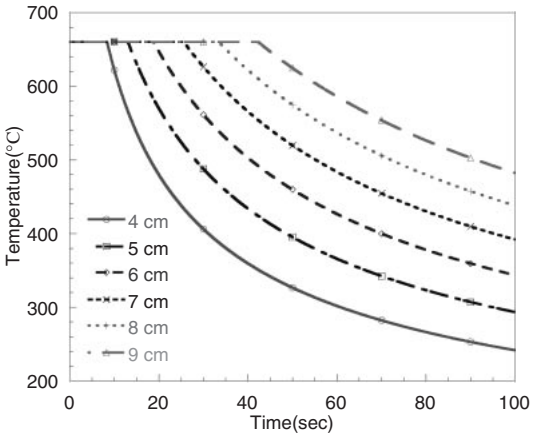

Fig. 4 Temperature distributions versus time of the Stefan problem for six different locations.

Table 1 Inverse-computed k_S and Cp_S of Stefan problem for different Δt's with $\Delta x = 0.01$ m.

Δt (second)	k_S (W/m·°C)	Cp_S (W/m^3·°C)	Relative error of k_S (%)	Relative error of Cp_S (%)
Exact	240.0	3000000	0	0
0.1	239.9	3004262	0.06	0.14
0.5	240.7	3014610	0.28	0.49
1.0	241.8	3028532	0.75	0.95

a casting process is not easy to control. In this study, the temperature data of the first and final grid points are used as the boundary conditions and the temperature data of the first time step are utilized as the initial condition.

The numerical experiment takes aluminum as the testing material, whose thermal conductivity, specific heat and latent heat are 240 W/m°C, 3000000 W/m^3°C and 96864 J/kg. The temperature distributions can be obtained from the exact solutions, which are shown in Fig. 4. In the figure, the cooling curves at six locations are illustrated.

Firstly, the inverse experiment uses different time step sizes, $\Delta t = 0.1$ s, 0.5 s and 1 s, to inversely calculate the heat conductivity and specific heat with constant space increment ($\Delta x =$ constant). The computed and exact (or given) thermal properties and the relative errors are shown in Table 1. From the table, it could be found that the inverse results are very closed to the exact ones and the larger Δt has the bigger error, but their differences are small.

Secondly, the experiment uses the different space increments, $\Delta x = 0.01$ m, 0.1 m and 0.5 m to inversely calculate the heat conductivity and specific heat at the fixed time step. The computed and exact (or given) thermal properties and the relative errors are shown in Table 2. In the table, the inverse results are very closed to the exact ones and the smaller Δx has the smaller error, but their differences are still small.

After the inverse predictions of thermal conductivity and specific heat, the effective specific heat method combined with the inverse estimation of specific heat is used to predict the latent heat. To test and verify the proposed method, the study uses the different sizes of artificial mushy zone, $\Delta T^* = 10$°C, 20°C and 30°C, to calculate the latent heat with $\Delta x = 0.01$ m and $\Delta t = 0.5$ second. The computed and exact

Table 2 Inverse-computed k_S and Cp_S of Stefan problem for different Δx's with $\Delta t = 0.1$ second.

Δx (m)	k_S (W/m·°C)	Cp_S (W/m^3·°C)	Relative error of k_S (%)	Relative error of Cp_S (%)
Exact	240.0	3000000	0	0
0.01	239.9	3004262	0.06	0.14
0.1	240.2	3009080	0.10	0.30
0.5	241.2	3021019	0.50	0.70

Table 3 Inverse-computed latent heat of Aluminum in the Stefan problem for different ΔT^*'s with $\Delta t = 0.5$ second and $\Delta x = 0.01$ m.

ΔT^* (°C)	From literature (J/kg)	Inverse-computed (J/kg)	relative error (%)
10	396864	400094	0.814
20	396864	403925	1.78
30	396864	434622	9.51

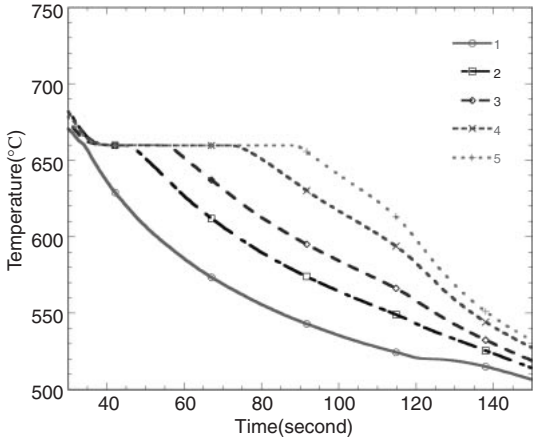

Fig. 5 Cooling curves of the aluminum cast in the sand mold.

latent heats and the relative errors are shown in Table 3. The computed latent heats are close to the exact one and the smaller ΔT^* has the smaller relative error. The relative error is lower than 2% when ΔT^* is equal to 10°C or 20°C, but the error goes up to 9.51% when ΔT^* is 30°C.

7.1.2 Numerical experimental results of Neumann problem

The cooling curves of Stefan problem (Fig. 4) are similar to those in the real casting experiment[14] (Fig. 5). However, in the Stefan problem, the temperature in the liquid region is equal to the melting temperature and there is no temperature variation. The temperature data taken from the liquid region cannot be used to predict the liquid thermal properties. Consequently, this work takes the temperature data from the Neumann problem to inversely calculate the thermal properties of liquid and solid.

The thermal properties are assumed to be constant in the Neumann problem and the inverse calculation. Aluminum is taken as the testing material. The cooling curves of the Neumann problem at six locations are illustrated in Fig. 6. In the figure, the cooling rates have little change at the solidification temperature (660°C) and the cooling curves do not stay at the temperature over a period of time.

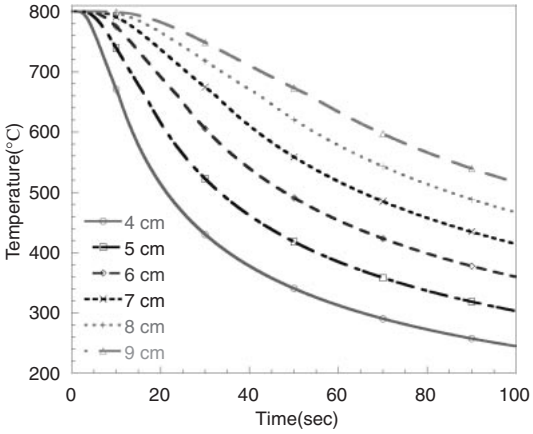

Fig. 6 Temperature distributions versus time of the Neumann problem.

Table 4 Inverse-computed k_S and Cp_S of the of Neumann problem for different Δt's with $\Delta x = 0.01$ m.

Δt (Second)	k_S (W/m·°C)	Cp_S (W/m^3·°C)	Relative error of k_S (%)	Relative error of Cp_S (%)
Exact	240	3000000	0	0
0.1	240.12	3047893.7	0.052	1.596
0.5	240.13	3047974.5	0.054	1.599
1.0	241.35	3062947.5	0.563	2.09

Table 5 Inverse-computed k_L and Cp_L of Neumann problem for different Δt's with $\Delta x = 0.01$ m.

Δt (Second)	k_L (W/m·°C)	Cp_L (W/m^3·°C)	Relative error of k_L (%)	Relative error of Cp_L (%)
Exact	96	2580000	0	0
0.1	96.88	2562939	0.91	0.66
0.5	96.91	2563866	0.95	0.63
1.0	96.96	2565062	1	0.58

The domain of Stefan problem is also semi-infinite. The number of temperature-measured points and the initial and boundary conditions taken for the inverse calculations are set to be the same as those in the Stefan problem. The numerical experiment of Neumann problem also chooses different conditions (different Δx's and Δt's) to test and verify the inverse method. The inversely computed thermal properties and relative errors are listed in Table 4, Table 5, Table 6 and Table 7. From those results, it could be found that their accuracies are as well as the Stefan's. Basically, the smaller Δx or Δt has the smaller relative error.

The predicted method of the latent heat of Neumann problem is a little different from that of Stefan problem, because the pouring temperature of Neumann problem is higher than the melting temperature T_f. This work takes a suitable temperature separation (ΔT^*) around T_f as the artificial mushy zone ($T_f - \Delta T^* < T < T_f + \Delta T^*$) to predicate the latent heat. With different sizes of artificial mushy zone ($\Delta T^* = 10$°C, 20°C and 30°C), $\Delta x = 0.01$ m and $\Delta t = 0.5$ second, the computed and exact latent heats and the relative errors are shown in Table 8. The computed latent heats are close to the exact one and the smaller ΔT^* has the smaller relative error. The relative error is lower than 1% when ΔT^* is equal to 10°C or 20°C, but the error goes up to 3.74% when ΔT^* is 30°C.

Table 6 Inverse-computed k_S and Cp_S of Neumann problem for different Δx's with $\Delta t = 0.1$ second.

Δx (m)	k_S (W/m·°C)	Cp_S (W/m^3·°C)	Relative error of k_S (%)	Relative error of Cp_S (%)
Exact	240	3000000	0	0
0.01	240.12	3047894	0.052	1.596
0.1	240.13	3047926	0.055	1.598
0.5	241.36	3062969	0.565	2.098

Table 7 Inverse-computed k_L and Cp_L of Neumann problem for different Δx's with $\Delta t = 0.1$ second.

Δx (m)	k_L (W/m·°C)	Cp_L (W/m^3·°C)	Relative error of k_L (%)	Relative error of Cp_L (%)
Exact	96	2580000	0	0
0.01	96.88	2562939	0.91	0.66
0.1	96.94	2564423	0.98	0.6
0.5	96.99	2565803	1.03	0.55

Table 8 Inverse-computed latent heat of Aluminum in the Neumann problem for different ΔT^*'s with $\Delta t = 0.5$ second and $\Delta x = 0.01$ m.

ΔT^* (°C)	From literature (J/kg)	Inverse-computed (J/kg)	relative error (%)
10	396864	398887	0.510
20	396864	400799	0.992
30	396864	411694	3.737

7.2 The results of the casting experiment

Some inverse methods need the boundary condition of specified heat flux, but it is not easy to measure the heat flux accurately in the experiment. In this work, the temperature-measured data are taken as the boundary conditions, which is easy to apply to the real casting experiment. In the casting experiment, the vertical thermal-insulated mold and its surrounding heater can reduce the radial heat transfer and the bottom water-cooling copper chill can enhance the axial heat transfer. These could help the casting experiment to simulate the one-dimensional heat transfer model.

In the casting experiment, the temperature distributions of the casting are measured by the five thermal couples that are located along the central line of the cylinder casting with the same distance between two neighboring thermal couples. Those temperature data are used to estimate the thermal conductivity, specific heat and latent heat. Because the thermal properties of the experimental materials are constant in the working temperature ranges of these experiments, the thermal properties are assumed to be constant in the inverse computation. This study uses aluminum, tin and A356 aluminum alloy as the experimental materials. The separation of the thermal couples that are measured every 0.5 second ($\Delta t = 0.5$ s) is 0.8 cm ($\Delta x = 0.8$ cm).

The cooling curves of aluminum cast in the green sand mold casting are shown in Fig. 5.[14] The cooling curves of

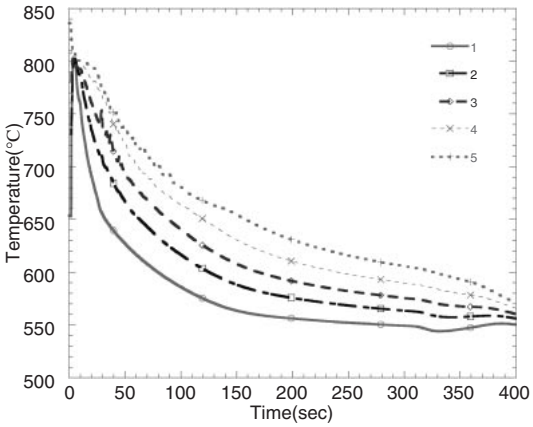

Fig. 7 Cooling curves of the aluminum cast in the vertical thermal-insulated mold.

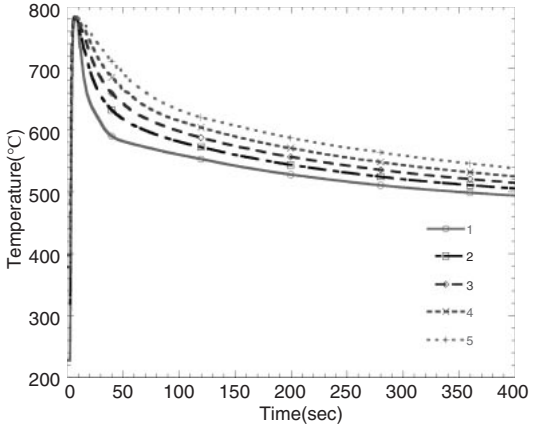

Fig. 8 Cooling curves of the A356 alloy cast in the vertical thermal-insulated mold.

aluminum and A356 aluminum alloy cast in the vertical thermal-insulated mold are illustrated in Fig. 7 and 8. In Fig. 5, the cooling curves stay at the melting temperature over a period of time, but the similar phenomenon can be found in Fig. 7 or 8. This is because the water-cooling copper chill can take much more heat than the sand mold.

7.2.1 Predicted liquid thermal conductivities and specific heats

To inversely calculate the liquid thermal properties, the temperature data are chosen from the region of large temperature variation in the cooling curve. At first, the inverse method is applied to pure metals. The temperature range used to predict the liquid thermal properties of aluminum is from 726°C to 796°C. The inverse-computed thermal conductivity is 96.94 W/m°C and the specific heat is 2564424 W/m^3°C. In this work, the reference thermal properties are taken from reference.[17,18] By comparing the predicted values with the reference ones, their relative errors are less than 1%. The temperature range of tin is from 327°C to 427°C and the inverse-computed thermal conductivity and specific heat are 31.65 W/m°C and 1712056 W/m^3°C, respectively. The relative error of the thermal conductivity is 2.012% and the error of the specific heat is 3.012%.

After the tests for the pure metal, the inverse method is applied to alloys. The temperature range of 90 mass%Sn-10 mass%Pb alloy is from 240°C to 277°C. The computed thermal conductivity is 40.95 W/m°C with the relative error of 6.09% and the specific heat is 8013047 W/m^3°C with the error of 0.715%. The temperature range of A356 aluminum alloy is from 700°C to 813°C. The computed thermal conductivity is 92.02 W/m°C with the relative error of 2.104% and the specific heat is 2939273 W/m^3°C with the error of 0.316%.

Table 9 Inverse-computed latent heat of the experimental data.

Metal	From literature (J/kg)	Inverse-computed (J/kg)	relative error (%)
Al	396864	408989	3.055
Sn	60697	63046	3.870

7.2.2 Predicted solid thermal conductivities and specific heats

At first, the inverse method is applied to pure metals. The temperature range used to predict the solid thermal properties of aluminum is from 427°C to 627°C. The inverse-computed thermal conductivity is 243.4 W/m°C and the specific heat is 3048278.3 W/m^3°C. Their relative errors are close to 1%. The temperature range of tin is from 127°C to 227°C and the inverse-computed thermal conductivity and specific heat are 59.97 W/m°C and 1640238 W/m^3°C, respectively. The relative error of the thermal conductivity is 0.616% and the error of the specific heat is 0.592%.

After the tests of the pure metal, the inverse method is applied to alloys. The temperature range of 90 mass%Sn-10 mass%Pb alloy is from 42°C to 87°C. The computed thermal conductivity is 55.716 W/m°C with the relative error of 6.132% and the specific heat is 7086116.97 W/m^3°C with the error of 0.005%. The temperature range of A356 aluminum alloy is from 435°C to 535°C. The computed thermal conductivity is 170.07 W/m°C with the relative error of 1.838% and the specific heat is 2265919 W/m^3°C with the error of 1.052%. From the inverse results stated above, it can be found that the inverse method is a good way to predict the thermal conductivities and specific heats of a casting material.

7.2.3 Predicted latent heat

The cooling curves of the aluminum and A356 aluminum alloy cast in the vertical thermal-insulated mold of (Fig. 7 and Fig. 8) are similar to those of Neumann problem, in which the phenomenon of the cooling curve staying at the melting point cannot be found. This work takes a suitable temperature separation (ΔT^*) around the melting temperature T_f as the artificial mushy zone ($T_f - \Delta T^* < T < T_f + \Delta T^*$) to predict the latent heat of pure metal. Table 9 indicates the computed latent heats of aluminum and tin and the relative errors compared with those form the literature. The relative errors are small and less than 4%.

Since an alloy does not have single melting temperature, it is not easy to inversely calculate its latent heat. In this work, the same method used for pure metal is applied to predict the latent heat of an alloy. For 90 mass%Sn-10 mass%Pb alloy, six reference melting temperatures are chosen between the liquidus and eutectic temperatures with $\Delta T^* = 10$°C or 16.5°C to estimate the latent heat, whose results are shown in

Table 10 Inverse-computed latent heat of Sn-10 mass%Pb alloy for different solidification points of reference with $\Delta T^* = 10°C$ and $L_f = 55960\,J/kg$ from literature.

The reference temperature point of solidification	Inverse-computed (J/kg)	Relative error (%)
T_L, 216°C	61589	10.06
$(3T_L + T_{eut})/4$, 208°C	61870	10.56
$(T_L + T_{eut})/2$, 200°C	58708	4.91
$(T_L + T_{eut})/2$, 200°C $\Delta T = 16.5°C$ = (freezing range)/2	54501	2.61
$(T_L + 3T_{eut})/4$, 192°C	60767	8.59
T_{eut}, 183°C	59430	6.20

Table 11 Inverse-computed latent heat of the A356 alloy experiment for different solidification points of reference with $\Delta T^* = 10°C$ and $L_f = 389000\,J/kg$ from literature.

The reference temperature point of solidification	Inverse-computed (J/kg)	Relative error (%)
T_L, 615°C	431294	10.872%
$(3T_L + T_{eut})/4$, 604°C	431097	10.822%
$(T_L + T_{eut})/2$, 593°C	401977	3.336%
$(T_L + T_{eut})/2$, 593°C $\Delta T = 22.5°C$ = (freezing range)/2	389698	0.179%
$(T_L + 3T_{eut})/4$, 582°C	412469	6.033%
T_{eut}, 570°C	403912	3.833%

Table 10. From the table, it is surprised to find that the relative errors for these six cases are not big. For A356 aluminum alloy, six reference melting temperatures are chosen between the liquidus and eutectic temperatures with $\Delta T^* = 10°C$ or 22.5°C to estimate the latent heat, whose results are shown in Table 11. Similar to Table 10, the relative errors for these six cases are not large. In Table 10 and 11, the reference melting temperature at the middle between the liquidus and eutectic temperatures with ΔT^* equal to one half of the freezing range has the smallest error.

8. Conclusion

In this paper, based on Yang's method, an inverse method is proposed to predict the solid and liquid thermal conductivities and specific heats simultaneously and then to estimate the latent heat with the effective specific heat method. The proposed method is tested and verified by taking the measured temperatures from the exact solutions of the Stefan and Neumann problems and the real casting experiments. From the results above, the following conclusions can be made:

(1) In the numerical experiments with the Stefan and Neumann problems, the computed thermal conductivities and specific heats and the latent heat are very close to the exact ones. The relative errors can be less than 2%.

(2) In the casting experiment, a thermal-insulated vertical mold with the bottom water-cooling copper chill is used to simulate the one-dimensional heat transfer for the proposed inverse method. The computed solid and liquid thermal conductivities and specific heats of aluminum, tin and A356 alloy are close to those from the literature. Most of the relative errors are less than 2%.

(3) In the casting experiments, the estimated latent of aluminum and tin are close to those from the literature. The latent heats of Sn-10 mass%Pb alloy and A356 alloy are predicted by using the same method of pure metal and the computed latent heats are consistent with the values taken from the literature. With the reference melting temperature at the middle between the liquidus and eutectic temperatures and ΔT^* equal to one half of the freezing range, the relative error can lower down to 2.6% for Sn-10 mass%Pb alloy and 0.18% for A356 alloy.

REFERENCES

1) K. S. and N. S. SIMA J. Contr. Optimiz **15** (1977) 785–802.
2) Y. M. Chen and L. Q. Liu: J. Comput. Phys. **43** (1981) 315–326.
3) C. H. Huang and M. N. Ozisik: Numerical Heat Transfer, Part A **20** (1991) 95–110.
4) O. M. Alifanov: J. of Engineering Physics **26** (1974) 471–476.
5) O. M. Alifanov and E. A. Artyukhim: J. of Engineering Physics **29** (1975) 934–938.
6) C. H. Huang and M. N. Ozisik: Numerical Heat Transfer, Part A **20** (1991) 95–110.
7) H. T. Chen and S. M. Chang: Int. J. Heat Mass Transfer **33** (1990) 621–628.
8) H. T. Chen and J. Y. Lin: Int. J. Heat Transfer **34** (1991) 1301–1308.
9) H. T. Chen and J. Y. Lin: Appl. Math. Modelling **15** (1991) 144–151.
10) S.-H. Zhong: Ph.D. thesis, Department of Resources Engineering, National Cheng Kung University, Taiwan (1992).
11) C. Y. Yang: Communications in Numerical Method in Engineering **13** (1997) 419–427.
12) C. Y. Yang: Applied Mathematical Modelling **22** (1998) 1–9.
13) K. G. Upadhya, D. M. Stefanescu, K. Lieu and D. P. Yeager: AFS Transaction **47** (1989) 61–66.
14) M.-Y. Guo: Graduated thesis, Department of Engineering Science, National Cheng Kung University, Taiwan (1999).
15) H. S. Carslaw and J. C. Jaeger: *Conduction of Heat in Solids*, 2nd ed., (Oxford, England 1959).
16) J. E. Kelly: Ph.D. thesis, Department of Mechanical and Industrial Engineering, University of Illinois at Urbana-Champaign, Illinois, U.S.A. (1989).
17) W. H. Cubberly: *American Society for Metals. Reference Publications*, Metals Park, 2nd edition, (Ohio, ASM 1983).
18) J. F. Shackelford, W. Ander and J. S. Park: *Materials Science and Engineering*, 2nd edition, (CRC press, Inc, Boca Raton, Floida, U.S.A. 1994).